$$V_o = 0.31\, V_B^* \qquad (4)$$

If the equation for diffusion coefficient is multiplied by V_B/V_o, then

$$D_{AB} = 0.088 \frac{V_B^{*4/3}}{N^{2/3}} \frac{RT}{\mu V_o} \frac{1}{V_A^{*2/3}} \qquad (5)$$

Akgerman and Gainer (1972*a*) have proposed a correlation for diffusion coefficients using absolute rate theory. This equation contains an exponential temperature dependence of the Arrhenius type. Akgerman and Gainer (1972*b*) compared this equation with that of Wilke-Chang (1955) and other available correlations and claimed that in most cases their (Akgerman-Gainer) correlation gives better predictions than all other correlations. In Table 1, Equation (5) is compared with experimental data and the Akgerman-Gainer correlation. It is clear that Equation (5) predicts diffusion coefficients with reasonable accuracy. This is especially true with solvents like cyclohexane and benzene, where there is quite significant increase in molal volume as the temperature increases. It should be noted that Equation (5) is much simpler to use than the Akgerman-Gainer equation. It should also be mentioned that Equation (5) should not be used for gases like hydrogen and helium (Hildebrand, 1971).

Equation (5) has also been tested on liquid-liquid systems, and the predictions are shown in Table 2. Unfortunately, the Akgerman-Gainer correlation is not very suitable for liquid-liquid systems (Akgerman-Gainer, 1972*a*); hence, comparison is made with the Wilke-Chang correlation which gives better predictions for liquid-liquid systems. The predictions are of reasonable accuracy. Hence, Equation (5) can be used for both gas-liquid and liquid-liquid systems.

The aim of the present work has been to derive an equation for predicting diffusion coefficients. It is preferable to use experimental values of viscosity rather than trying to correlate viscosity to molal volumes through the Batschinski equation. The derived equation is reasonably successful at lower temperatures. It is quite possible that at higher temperatures this simplified approach may not be entirely correct and that contributions from an entirely different mechanism may become important. Ertl and Dullien (1973) show that diffusion depends to a greater extent than viscous flow on volume expansion. The work of Gotoh (1976) on free volumes in liquids shows that the pore dimensions in water are less than the solute molecular diameter. In such cases, an activation energy concept may be necessary. This is entirely speculative, and further experimental work, especially at higher pressures and temperatures, is necessary to delineate these mechanisms.

NOTATION

D = diffusion coefficient
N = Avagadro number
R = universal gas constant
T = temperature
V = molal volume

Greek Letters

μ = viscosity

Subscripts

A = solute
B = solvent
o = intrinsic value

Superscript

* = critical property

LITERATURE CITED

Akgerman, A., and J. L. Gainer, "Diffusion of gases in Liquid," *Ind. Eng. Chem. Fundamentals*, **11**, 373 (1972*a*).

———, "Predicting Gas-Liquid Diffusivities," *J. Chem. Eng. Data*, **17**, 372 (1972*b*).

Batschinski, A. J., "Untersuchungen über die innere Reibung der Flüssigkeiten," *Z. Physik. Chem.*, **84**, 643 (1913).

Dullien, F. A. L., "Predictive Equations for Self-Diffusion in Liquids: a Different Approach," *AIChE J.*, **18**, 62 (1972).

Ertl, H., and F. A. L. Dullien, "Self-Diffusion and Viscosity of Some Liquids as a Fuction of Temperature," *ibid.*, **19**, 1215 (1973).

Gotoh, K., "Solubilities of Nonreacting Gases in Liquids from the Free-Volume Theory," *Ind. Eng. Chem. Fundamentals*, **15**, 269 (1976).

Hayduk, W., and W. D. Buckley, "Effect of Molecular Size and Shape on Diffusivity in Dilute Solutions," *Chem. Eng. Sci.*, **27**, 1997 (1972).

Hildebrand, J. H., "Motions of Molecules in Liquids: Viscosity and Diffusivity," *Science*, **174**, 490 (1971).

———, and R. H. Lamoreaux, "Diffusivities of Gases in Liquids," *Proc. Natl. Acad. Sci. USA*, **71**, 3321 (1974).

Lynch, D. W., "Gas-Liquid Diffusivities Wetted Sphere Absorber," Ph.D. thesis, Monash Univ., Australia (1974).

Wilke, C. R., and P. Chang, "Correlation of Diffusion Coefficient in Dilute Solution," *AIChE J.*, **1**, 264 (1955).

Manuscript received January 11, and accepted February 23, 1977.

Adsorption Rates of Oxygen in Aqueous Slurries of Activated Carbon

HIROO NIIYAMA

and

J. M. SMITH

University of California
Davis, California 95616

A method has recently been developed (Niiyama and Smith, 1976) for evaluating mass transfer and adsorption rates in three-phase slurry reactors by analyzing breakthrough curves in the effluent gas stream. Since slurry systems have been proposed for removing pollutants by oxidation with gaseous oxygen, and since the rate of oxygen adsorption can significantly influence the rate of oxidation (Komiyama and Smith, 1975), we have used the new method to determine mass transport and intrinsic adsorption rate parameters for oxygen in aqueous slurries of carbon particles. The same apparatus and experimental techniques were employed as used in the earlier work, where the theory was developed and applied to data for adsorption of nitric oxide in carbon slurries. Hence, this note emphasizes only the results, which show that bubble-to-liquid mass transfer, intraparticle diffusion, and intrinsic adsorption at an interior site can all affect the overall ad-

Hiroo Niiyama is on leave from Tokyo Institute of Technology, Japan.

sorption process. The results also show that the method is well suited for the measurement of the intrinsic rate constant for adsorption.

METHOD

Consider a system in which gas bubbles are introduced through a disperser tube into the bottom of an agitated slurry. A step function of oxygen is fed into the helium stream entering the slurry, and the oxygen breakthrough curve (BTC) is measured in a detector sensing the oxygen concentration in the gas leaving the slurry. The process is supposed to consist of the following steps and characteristic rate coefficients: liquid side, bubble-to-bulk liquid mass transfer (k_L), liquid-to-particle surface transport (k_s), intraparticle diffusion (D_e), and adsorption at an interior site (k_{ads}). For this model, it was shown (Niiyama and Smith, 1976) that the first absolute and second central moments are related to these coefficients by

$$\mu'_{1,D} - \mu'_{1,d.v.} = \frac{m_s K + 1}{H}\left(\frac{V_L}{Q}\right) \tag{1}$$

$$\mu_{2,D} - \mu_{2,d.v.} = \frac{2}{H}\left[\left(\frac{R}{5D_e a_s} + \frac{1}{k_s a_s}\right)\left(m_s\frac{\beta}{\rho_p} + m_s K\right)^2 + \frac{m_s K^2}{k_{ads}}\right]\frac{V_L}{Q} + \left(\frac{m_s K + 1}{H}\right)^2\left(\frac{1+e^{-\alpha L}}{1-e^{-\alpha L}}\right)\left(\frac{V_L}{Q}\right)^2 \tag{2}$$

where $\mu'_{1,D}$ and $\mu_{2,D}$ are the moments measured at the detector and $\mu'_{1,d.v.}$ and $\mu_{2,d.v.}$ are correction terms for the moments in the dead volumes between feed injection valve and entrance to slurry and between upper liquid level of the slurry and detector. α is given by

$$\alpha = \frac{k_L a_B}{v_B V_B H} = \frac{k_L a_B}{HL}\left(\frac{V_L}{Q}\right) \tag{3}$$

The main assumptions made in deriving Equations (1) and (2) are: the adsorption from liquid to carbon surface is reversible and linear, the gas bubbles travel through the slurry in plug flow, and the liquid phase is completely mixed. The validity of the second and third assumptions are discussed in the earlier paper, while the first assumption requires experimental verification.

Values of the moments at the detector are related to the BTC by the equations

$$\mu'_{1,D} = \frac{1}{C_{go}}\int_0^\infty (C_{go} - C_g)\,dt \tag{4}$$

$$\mu_{2,D} = \frac{2}{C_{go}}\int_0^\infty (C_{go} - C_g)\,t\,dt - (\mu'_{1,D})^2 \tag{5}$$

TABLE 1. OPERATING CONDITIONS

Volume of water in slurry	= 1 015 cm³
Weight of carbon in slurry	= 200 g
m_s	= 0.197 g/cm³
O_2 concentration in the feed stream:	
for equilibrium data:	2 to 20%
for rate data:	10%
Gas flow rate:	3.33 to 10 cm³/s (at 25°C, 1 atm)
Impeller speed:	670 ± 40 rev/min
Temperature:	5 ± 0.3°C, 26 ± 1.0°C
Pressure:	1 atm

Carbon particle radius: 0.0015, 0.040, 0.070, 0.095 cm

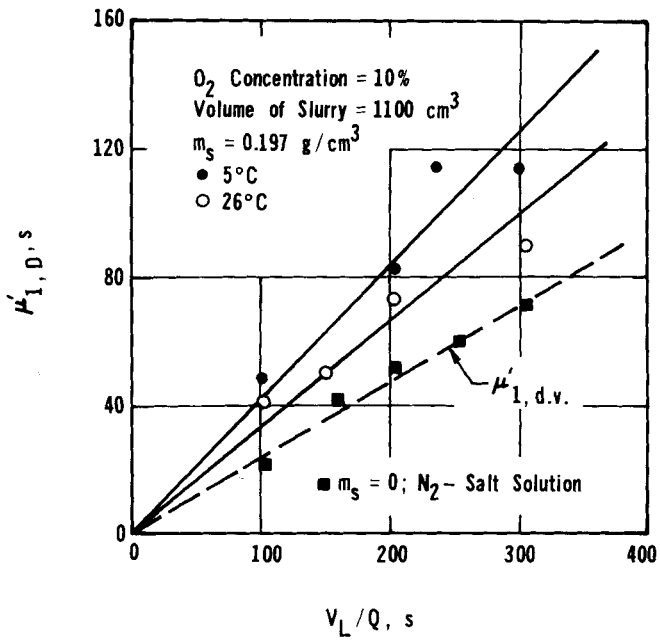

Fig. 1. First-moment results.

The procedure is to calculate $\mu'_{1,D}$ and $\mu_{2,D}$ from the measured BTC. The dead-volume contributions, $\mu'_{1,d.v.}$ and $\mu_{2,d.v.}$ are determined similarly from BTC for a nearly insoluble chemical system in the same apparatus. For this we used the results of measurements for nitrogen bubbling through a saturated sodium chloride solution, as obtained in the earlier work. First-moment data for water alone ($m_s = 0$) and for slurries can then be used with Equation (1) to determine H and K. Next, second-moment data for various gas flow rates (Q), particle sizes, and for two temperatures were used with Equation (2) to obtain $k_L a_B$, D_e, and k_{ads}.

The slurry vessel was a Pyrex cylinder 10 cm I.D., 13 cm high, equipped with impeller and baffles. Type BPL carbon supplied by Calgon Corporation was used. This material has a particle density (ρ_p) of 0.85 g/cm³, porosity (β) of 0.60, and BET surface area of about 1 100 m²/g. The gas stream emerged as bubbles through a fritted glass disperser disk located about 12 cm below the top of the slurry liquid. Complete description of the bubble properties, apparatus, and operating procedure are described by Niiyama and Smith (1976), and the range of operating conditions are given in Table 1.

EQUILIBRIUM RESULTS

Equation (1) shows that $\mu'_{1,D} - \mu'_{1,d.v.}$ is proportional to V_L/Q for BTC runs at constant temperature and constant V_L. Since $\mu'_{1,d.v.}$ is also proportional to V_L/Q for such runs, $\mu'_{1,D}$ data should give a straight line through the origin. This is illustrated in Figure 1 for a step function input concentration of 10% oxygen. Results at both temperatures are shown as well as the first-moment data for the dead volume $\mu'_{1,d.v.}$ determined from runs with the nitrogen-sodium chloride solution system. Such data for various step function concentrations were used to obtain K from Equation (1). First H was obtained from BTC measurements for water alone using Equation (1) with $m_s = 0$. The results for both the solubility (H) and adsorption isotherm (K) are shown in Figure 2. Henry's law constant was 41.3 and $K = n/C_L = 10.8$ cm³/g at 26°C. The solubility data in the Literature (Linke, 1965) are also shown in Figure 2. The adsorption capacity for oxygen is somewhat higher than that for nitric oxide ($K = 6.9$ cm³/g at 26°C) as determined in the earlier work.

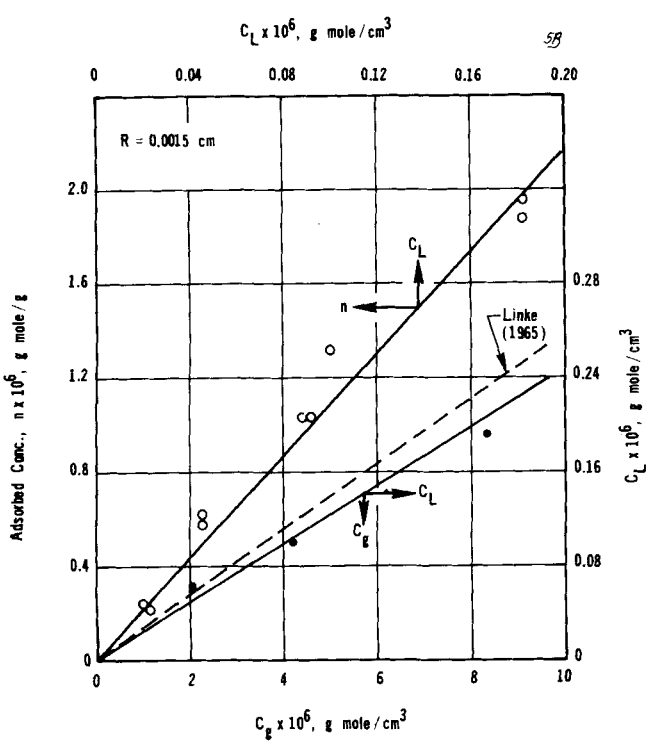

Fig. 2. Adsorption and absorption isotherms for the oxygen-water-carbon system at 26°C.

For the subsequent analysis, the key feature of the equilibrium results is that the adsorption isotherm in Figure 2 is linear. To test for reversibility, a desorption run was made after equilibrium adsorption had been reached. When fresh carbon was used, the measured desorption for the first run was about 10% less than the amount of oxygen adsorbed. However, subsequent runs with the same carbon showed complete desorption, indicating that the highly active sites on which irreversible adsorption occurred had been occupied during the initial run. The results that follow refer to the reversible adsorption runs.

Comparison of the data in Figure 1 for 5° and 26°C indicates a heat of adsorption of about 2.9 kcal/mole.

SECOND-MOMENT ANALYSIS

Rearrangement of Equation (2) to the form

$$(\mu_{2,D} - \mu_{2,\text{d.v.}})\frac{Q}{V_L} = \frac{2}{H}\left[\left(\frac{R}{5D_e a_s} + \frac{1}{k_s a_s}\right)\left(m_s\frac{\beta}{\rho_p} + m_s K\right)^2\right] + \frac{m_s K^2}{k_{\text{ads}}}\Bigg] + \left(\frac{m_s K + 1}{H}\right)^2\left(\frac{1 + e^{-\alpha L}}{1 - e^{-\alpha L}}\right)\frac{V_L}{Q} \quad (6)$$

shows the dependence of the operating conditions on each of the contributions to the second moment. The last term involving k_L is the only one that depends upon gas flow rate. Since both a_B and V_B are proportional to Q, Equation (3) indicates that αL is independent of Q. Hence, a plot of the left side of Equation (6) vs. V_L/Q should be a straight line whose intercept I is equal to the three contributions to $\mu_{2,D}$ due to D_e, k_s, and k_{ads}, while the slope establishes $k_L\, a_B$. For spherical particles $a_s = 3m_s/\rho_p R$, which gives values from 493 to 8.9 cm^{-1}, depending on particle size. From the data and correlations of Furusawa and Smith (1973), the corresponding range of k_s is from 0.030 to 0.021 cm/s. With these values, the term involving $k_s\, a_s$ is so small that it is within the experimental accuracy

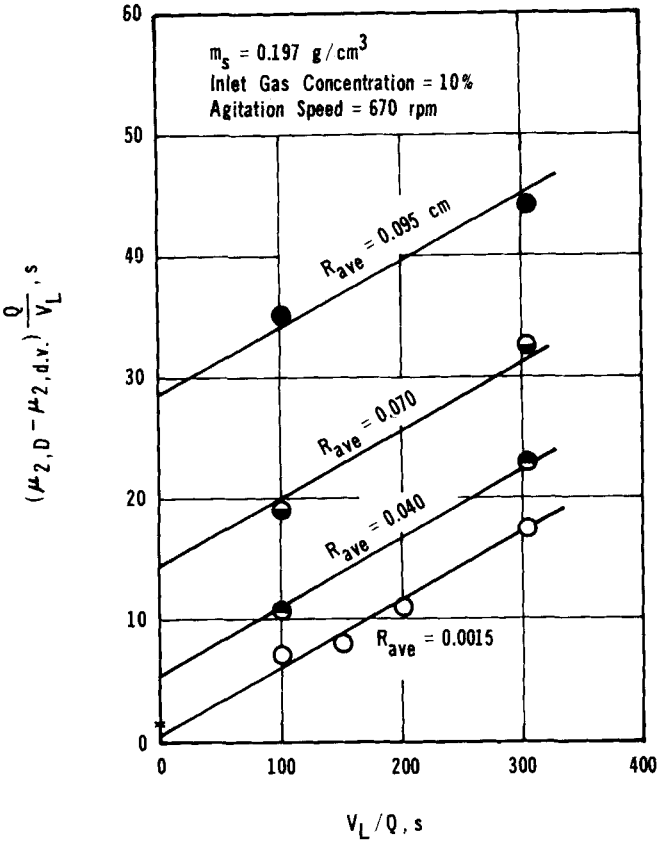

Fig. 3. Second-moment results for the oxygen-water-carbon system at 26°C.

of measuring the left side of Equation (6). Then the intercept I may be written

$$I = \frac{2m_s}{H}\left[\frac{\rho_p}{15\,D_e}\left(\frac{\beta}{\rho_p} + K\right)^2 R^2 + \frac{K^2}{k_{\text{ads}}}\right] \quad (7)$$

Equation (7) shows that the intercept should be linear in R^2 and that a plot of I vs. R^2 would have a slope from which D_e can be obtained and an intercept which determines k_{ads}.

This method of analysis was used with second-moment results to evaluate $k_L\, a_B$, D_e, and k_{ads}.

Bubble-to-Liquid Mass Transfer

Figure 3 shows the data at 26°C plotted as $(\mu_{2,D} - \mu_{2,\text{d.v.}})\, Q/V_L$ vs. V_L/Q for different particle sizes. From the slope of the lines and for $Q = 3.33$ cm^3/s, $k_L\, a_B = 0.026$ s^{-1}. The previously obtained result for nitric oxide was 0.021 s^{-1}. The two values would be expected to be similar, since physical properties of nitric oxide and oxygen are similar and the apparatus was the same. An evaluation of k_L separately is less accurate because of the difficulty in obtaining an accurate value for a_B. From the earlier measurements of bubble sizes and other measured information, a_B was estimated to be 0.081 cm^{-1}, giving k_L = 0.33 cm/s. This relatively high value may be due to a higher gas holdup in the slurry than that corresponding to plug flow of bubbles and due to omission of mass transfer between the upper surface of the slurry liquid and the gas phase. For the evaluation of k_s, D_e, or k_{ads}, only the product $k_L\, a_B$ is required. It can be shown (Niiyama and Smith, 1976) that this product is independent of the mixing state (plug flow to complete mixing) of the gas bubbles for the conditions of the experiments.

Intraparticle Diffusion

The intercepts I from Figure 3 are plotted vs. R^2 in Figure 4. From the slope of the line, D_e is 2.0 × 10^{-5}

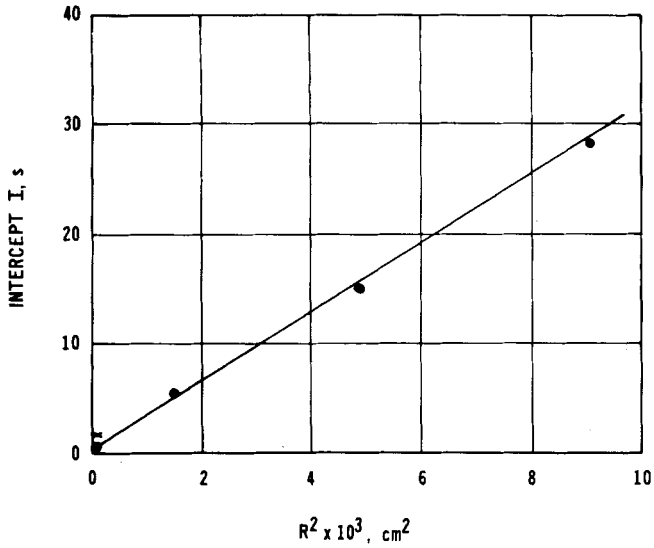

Fig. 4. Effect of particle size on second moment at 26°C.

cm^2/s. Since the molecular diffusivity (D) of oxygen in water is 2.60×10^{-5} cm^2/s (Reid and Sherwood, 1966), such a value for D_e suggests a tortuosity factor ($\gamma = \beta D/D_e$) of about 0.7. While surface migration could be responsible for the low γ, other factors may be involved. For example, in the very small pores of the activated carbon (average pore radius = 13Å), the usual molecular diffusivity may not be applicable because of interaction between the polar oxygen molecules adsorbed and in the water phase.

Adsorption Rate

The intercept of the line for the smallest particle size ($R = 0.0015$ cm) in Figure 3 is nearly zero. From Equation (7) it is concluded that both intraparticle diffusion and adsorption offer negligible resistance to the overall process at 26°C. This is also apparent from the fact that the point for the smallest particle size in Figure 4 has a near zero ordinate. For this reason it is not possible to measure accurately the rate constant at 26°C. However, the second-moment results at the lower temperature (5°C) for $R = 0.0015$ cm do yield a significant intercept, as seen in Figure 5. At 5°C, $K = 15.8$ cm^3/g from the slope of the line in Figure 1, and Linke (1965) gives $H = 22.8$ for oxygen. Equation (7) shows that the intercept in Figure 5 is equal to $2m_s K^2/(H k_{ads})$ for these smallest particles, since the intraparticle diffusion contribution is negligible. From the values of K and H at 5°C, k_{ads} is 0.32 cm^3/(g)(s).

Komiyama and Smith (1975) in their study of the oxidation of sulfur dioxide, using a slurry of the same activated carbon particles as catalyst, concluded that the rate of adsorption of oxygen controlled the oxidation rate. If we assume that their rate of reaction is equal to the rate of oxygen adsorption, a value of $k_{ads} = 2.25$ cm^3/(g)(s) is obtained at 25°C. This corresponds to the intercept value designated by a cross in Figures 3 and 4. The approximate agreement of this result with the line in Figure 4 provides additional evidence that intraparticle diffusion is negligible for $R = 0.0015$ cm and that the rate of adsorption is large at 26°C.

These results suggest that the dynamic method used here can be useful for evaluating intrinsic adsorption rates in slurries, provided that such rates are not so large as to be masked by mass transfer contributions to the second moment. Since the previous results for nitric oxide were for the same activated carbon, the comparison of intrinsic rate constants for nitric oxide and oxygen adsorption is instructive. For nitric oxide, k_{ads} at 26°C was 0.058 cm^3/(g)(s), while the value for oxygen, even at the lower temperature of 5°C, is six times larger [0.32 cm^3/(g)(s)]. There is other evidence that nitric oxide has low adsorption rates, as for example in the review of Shelef and Kummer (1971) on adsorption and heterogeneous catalytic reactions of nitric oxide. It was proposed there that considerations of potential energy surfaces and absolute rate theory indicate that nitric oxide can exhibit a low transmission coefficient.

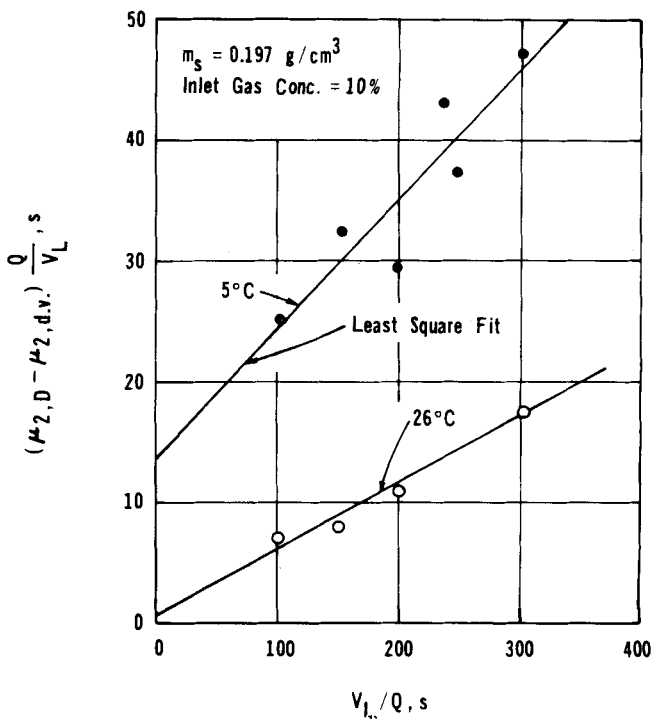

Fig. 5. Second-moment data at 5°C and 26°C for smallest particles ($R = 0.0015$ cm).

Our results show that the gas flow rate, particle radius, and temperature can affect the overall adsorption of oxygen in a three-phase slurry reactor. At the lower temperature and for small particle sizes, $k_L a_B$ and k_{ads} have the greatest effect on the overall adsorption rate. For larger particle sizes and the higher temperature (26°C), the influence of $k_L a_B$ and D_e predominates. Operation with lower values of m_s and higher gas flow rates, while not covered in our experiments, would result in $k_s a_s$ becoming significant, while $k_L a_B$ would become less important.

NOTATION

a_B = surface area of bubbles per unit volume of bubble and solid free liquid, cm^{-1}
a_s = outer surface area of particles per unit volume of bubble and solid free liquid, cm^{-1}
C_g = gaseous concentration of oxygen at the detector (C_g) or in the feed (C_{go}), mole/cm^3
C_L = concentration of oxygen in liquid, mole/cm^3
D = molecular diffusivity of oxygen in water, cm^2/s
D_e = effective intraparticle diffusivity, cm^2/s
H = Henry's law constant, $H = C_g/C_L$
K = adsorption equilibrium constant, cm^3/g of carbon
k_{ads} = intrinsic adsorption rate constant, cm^3/(g)(s)
k_L = bubble-to-liquid mass transfer coefficient, cm/s
k_s = liquid-to-particle mass transfer coefficient, cm/s
L = height of slurry above disperser disk, cm
m_s = mass of carbon particles per unit volume of bubble and solid free liquid, g/cm^3
n = concentration of adsorbed oxygen, moles/g

Q = gas flow rate at 25°C and 1 atm, cm³/s
R = radius of spherical particle, cm
t = time, s
V_B = bubble volume per unit volume of bubble and solid free liquid
V_L = total volume of liquid in the vessel, cm³
v_B = vertical bubble velocity, cm/s

Greek Letters

α = bubble-to-liquid rate parameter defined by Equation (3), cm^{-1}
β = particle porosity
γ = tortuosity factor
$\mu'_{1,D}$ or $\mu'_{1,d.v.}$ = first absolute moment measured at the detector, for slurry system or for dead volume, respectively, s
$\mu_{2,D}$ or $\mu_{2,d.v.}$ = second central moment measured at the detector for slurry system or for dead volume, respectively, s^2
ρ_p = particle density, g/cm³

LITERATURE CITED

Furusawa, T., and J. M. Smith, "Fluid-Particle and Intraparticle Mass Transfer Rates in Slurries," *Ind. Eng. Chem. Fundamentals*, **12**, 197 (1973).

Komiyama, H., and J. M. Smith, "Sulfur Dioxide Oxidation in Slurries of Activated Carbon, I. Kinetics," *AIChE J.*, **21**, 664 (1975).

Linke, W. F., *Solubilities*, American Chemical Society, Washington, D. C. (1965).

Niiyama, H., and J. M. Smith, "Adsorption of NO in Aqueous Slurries of Activated Carbon," *AIChE J.*, **22**, 961 (1976).

Reid, R. G., and T. K. Sherwood, *The Properties of Gases and Liquids*, 2 ed., McGraw-Hill, New York (1966).

Shelef, M., and J. T. Kummer, "The Behavior of Nitric Oxide in Heterogeneous Catalytic Reactions," *Chem. Eng. Progr. Symposium Ser.*, **67**, 74 (1971).

Manuscript received January 5, and accepted February 21, 1977.

Analysis of Two-Dimensional Air-Bubble Plumes

NIHAD A. HUSSAIN

Professor of Mechanical Engineering
San Diego State University
San Diego, California 92182

and

BALBIR S. NARANG

Associate Professor of
Aerospace Engineering
San Diego State University
San Diego, California 92182

In recent years, air-bubble systems have been applied successfully for many purposes, such as prevention of ice formation in lakes, as barriers against saltwater intrusion in rivers and lakes, for stopping the spreading of oil spills on water surface, for reduction of underwater explosion waves, and for aeration in water purification and waste treatment plants.

Two dimensional air-bubble plumes will exist when air is released from either a perforated tube or a tube with a longitudinal slot submerged in water. No suitable analytical model has been developed so far to describe the two-dimensional, two-phase plume when the density difference of the fluid inside the jet and that of the surrounding fluid, such as in the air-liquid case, is very large.

The purpose of this study is to extend the two-phase axisymmetric jet model, developed by Hussain and Siegel (1976), to the two-dimensional case. The proposed entrainment process, to account for the contributions to the entrainment by the outer liquid flow, the bubble wakes, and the rising air bubbles, is similar to that of Hussain and Siegel (1976).

ANALYSIS

The two-dimensional, two-phase jet considered here is similar to that of Figure 1 of Hussain and Siegel except that the circular orifice is replaced by a slot or a row of orifices. The flow field is assumed to be steady, isothermal, and fully turbulent. The density of the liquid is assumed constant, while the gas density is assumed to vary according to the ideal gas law. As in the work of Hussain and Siegel (1976), no attempt has been made to analyze the jet's turning zone when it reaches the liquid surface. It is also assumed that the gas leaves the submerged pipe with a negligible upward momentum. The bubbles are assumed to be sufficiently large so that their drag is fully turbulent, and hence they rise at constant terminal velocity relative to the liquid. The local bubble velocity is assumed equal to the local liquid velocity plus the bubble terminal velocity.

Gas Continuity

It is assumed that in the central region of the jet, bubbles are rising in a chain bubble fashion and that $1/(K+1)$ of the vertical height is occupied by the gas bubbles and $K/(K+1)$ is occupied by the liquid wake. This is shown in Figure 1. For a fixed gas flow rate, the mass flow rate M_g of the gas at any depth x can be written as

$$M_g = \int_o^{a_c} \frac{2}{K+1} U_g \rho_g dy = \text{constant} \qquad (1)$$